RSC Advances

PAPER

View Article Online
View Journal | View Issue

Cite this: *RSC Adv.*, 2019, **9**, 26126

The synthesis of a ^{99m}Tc-labeled tetravalent targeting probe upon isonitrile coordination to $^{99m}Tc^{I}$ for enhanced target uptake in saturable systems†

Yuki Mizuno,[ab] Tomoya Uehara,[a] Chun-wei Jen,[a] Hiromichi Akizawa*[b] and Yasushi Arano[a]

Received 8th June 2019
Accepted 11th August 2019

DOI: 10.1039/c9ra04311j

rsc.li/rsc-advances

The presence of excess unlabeled ligands in the injectate hinders the target uptake of ^{99m}Tc-labeled targeting vectors. To address the issue, we previously developed a chemical design which provides a ^{99m}Tc-labeled trivalent RGD probe upon CN-βAla-Gly-Gly-c(RGDfK) (L_β) coordination to $[^{99m}Tc][Tc(CO)_3]^+$ core at pH 6.0. In this study, we extended our coordination mediated synthesis of the trivalent RGD probe to that of a tetravalent one. Our initial attempts reacting L_β with $[^{99m}Tc][Tc(CO)_3]^+$ core at pH 8.0 failed to provide $[^{99m}Tc][Tc(CO)_2(L_\beta)_4]^+$ due to the formation of multiple side products. A γ-aminobutylic acid (GABA) based isonitrile ligand CN-GABA-Gly-Gly-c(RGDfK) (L_G), on the other hand, avoided the side reaction and selectively provided $[^{99m}Tc][Tc(CO)_2(L_G)_4]^+$ (^{99m}Tc-$[L_G]_4$) at pH 8.0. ^{99m}Tc-$[L_G]_4$ exhibited higher binding affinity to integrin $\alpha_v\beta_3$ than its unlabeled ligand, and visualized U87MG tumor without tedious post-labeling purification. These results indicate that the metal coordination-mediated syntheses of ^{99m}Tc-labeled multivalent probes have been successfully applied to a tetravalent one, which would allow a wider range of choices for designing novel ^{99m}Tc-labeled multivalent probes of high *in vivo* target uptake.

Introduction

Medical applications of metallic radionuclides have been rapidly expanding due to their unique roles in clinical nuclear medicine.[1–5] Metallic radionuclides emitting γ photon or β^+ particles are used for clinical nuclear imaging based on single photon emission computed tomography (SPECT) or positron emission tomography (PET), respectively, whereas ones emitting β^- or α particles are used for internal radiotherapy of malignant tumors. To achieve specific delivery of metallic radionuclides to target tissues such as cancer, peptides or antibody fragments which have high affinity to target molecules are often used as a targeting vector.[6] Since these molecules cannot form stable complexes with metallic radionuclides, they need to be modified with proper chelating agents, and carefully designed chelator-vector conjugates (hereafter referred as "ligands") should be employed for radiolabeling reactions (Fig. 1a).[7] Owing to the extremely low concentration of metallic radionuclides (for example, ^{99m}Tc < 1 μM (ref. 8)), however, these complexation reactions need to be performed with excess ligands (≈100 μM) to ensure high radiochemical yields in a short reaction time. As a result, the reaction solutions would contain not just the objective radiolabeled compounds but also excess unlabeled ligands (Fig. 1a). Upon the injection of these solutions into subjects, the target uptakes of the radiolabeled compounds would be competitively inhibited by the excess unlabeled ligands due to their similar binding affinities to target molecules (Fig. 1a).[9]

To circumvent the issue, our group has developed a novel chemical design concept of metal coordination mediated multivalency using the combination of $[^{99m}Tc][Tc^{I}(CO)_3]^+$ core and isonitrile ligands (Fig. 1b).[10,11] To test the validity of this design concept, we selected c(RGDfK) peptides as a model targeting vector, which has high affinity and specificity to integrin $\alpha_v\beta_3$.[12] $[^{99m}Tc][Tc^{I}(CO)_3(OH_2)_3]^+$ was firstly prepared as a labeling precursor, whose water molecules were then substituted by CN-βAla-Gly-Gly-c(RGDfK) (Fig. 2, L_β), a monovalent RGD ligand, at slightly acidic conditions (pH 6.0), providing $[^{99m}Tc][Tc^{I}(CO)_3(L_\beta)_3]^+$ (Fig. 2, ^{99m}Tc-$[L_\beta]_3$), a ^{99m}Tc-labeled trivalent RGD probe. ^{99m}Tc-$[L_\beta]_3$ exhibited higher binding affinity to integrin $\alpha_v\beta_3$

[a]*Laboratory of Molecular Imaging and Radiotherapy, Graduate School of Pharmaceutical Sciences, Chiba University, 1-8-1 Inohana, Chuo-ku, Chiba 260-8675, Japan*

[b]*Laboratory of Physical Chemistry, Showa Pharmaceutical University, 3-3165 Higashi-Tamagawagakuen, Machida, Tokyo 194-8543, Japan. E-mail: aki@ac.shoyaku.ac.jp*

† Electronic supplementary information (ESI) available: HPLC methods, synthesis scheme of the compounds **8a**, **8b**, **16**, stability of M-$[L_\beta']_3$ (M = $^{185/187}$Re and ^{99m}Tc) at pH 6.0, *in vitro* stability of ^{99m}Tc-$[L_G]_4$, competitive inhibition curves of the tested compounds, MS, ^{1}H-NMR, ^{13}C-NMR, IR, and/or purity check of key compounds. See DOI: 10.1039/c9ra04311j

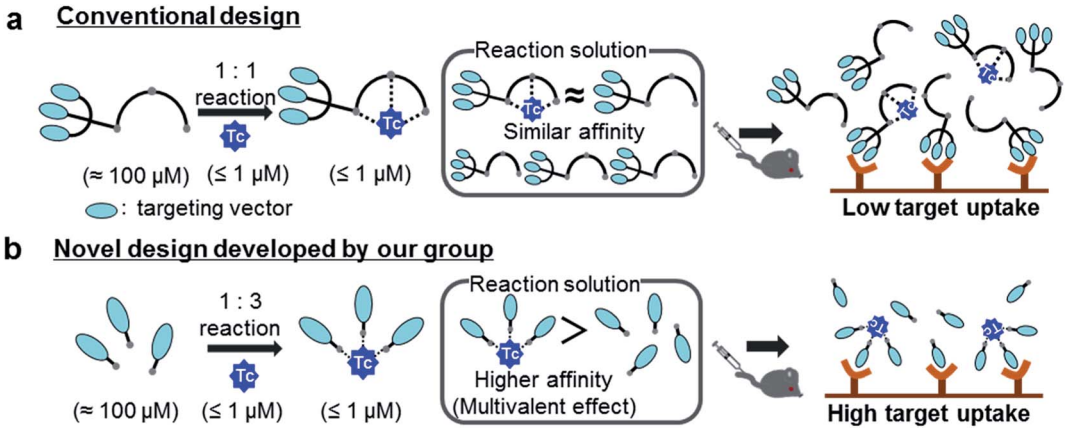

Fig. 1 Schematic illustration of a conventional and a novel chemical design. (a) The reaction solution, along with the ^{99m}Tc-labeled probe, contains excess unlabeled ligands whose binding affinity to a target molecule is similar to that of the ^{99m}Tc-labeled probe. Upon injection into subjects without post-labeling purification, the target uptake of the ^{99m}Tc-labeled probe is competitively inhibited by the presence of the unlabeled ligands. (b) The ^{99m}Tc-labeled trivalent probe would exhibit enhanced target binding affinity compared with its unlabeled ligand due to the multivalent effect. This superior target binding affinity of the ^{99m}Tc-labeled probe would enable high *in vivo* target uptake of the radiotracer without post-labeling purification. Adapted with permission from Mizuno *et al.*, Purification-Free Method for Preparing Technetium-99m-Labeled Multivalent Probes for Enhanced in Vivo Imaging of Saturable Sytems, *J. Med. Chem.*, 2016, **59**, 3331–3339. Copyright 2016 American Chemical Society.[10]

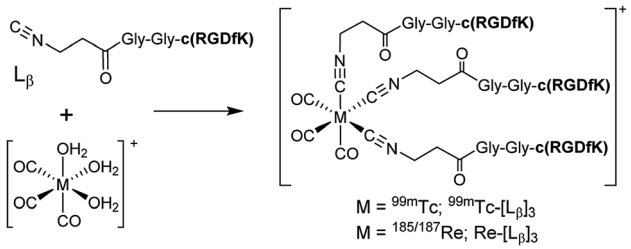

Fig. 2 Reaction scheme of L_β and $[^{99m}Tc][Tc^{I}(CO)_3(OH_2)_3]^+$. A ^{99m}Tc-labeled trivalent RGD probe $[^{99m}Tc][Tc^{I}(CO)_3(L_\beta)_3]^+$ (^{99m}Tc-$[L_\beta]_3$) is generated from a reaction between $[^{99m}Tc][Tc^{I}(CO)_3(OH_2)_3]^+$ and L_β in the molar ratio of 1 to 3.

compared with its unlabeled monovalent ligand (L_β), due to the multivalent effect.[13–15] This superior target binding affinity of ^{99m}Tc-$[L_\beta]_3$ enabled its high *in vivo* tumor uptake even in the presence of excess unlabeled ligands (Fig. 1b). We also demonstrated the applicability of this design concept to ^{99m}Tc-labeled bivalent probes[16] and ^{67}Ga-labeled trivalent ones[17] using D-penicillamine and Schiff base as a chelating molecule, respectively.

Our design concept would not be restricted to bivalent or trivalent probes but could be applied to other valent probes such as tetravalent or hexavalent ones. For example, it was reported that the reaction of methoxy-isobutyl-isonitrile (Fig. 3, MIBI) with $[^{99m}Tc][Tc^{I}(CO)_3(OH_2)_3]^+$ at basic conditions generated $[^{99m}Tc][Tc^{I}(CO)_2(MIBI)_4]^+$, where one CO molecule in $[^{99m}Tc][Tc^{I}(CO)_3(MIBI)_3]^+$ was further substituted by another MIBI molecule.[18] This result indicates that the preparation of ^{99m}Tc-labeled tetravalent RGD probes would be possible by employing appropriate isonitrile ligands and reaction conditions. However, it is still unknown if any isonitrile ligands could provide ^{99m}Tc-labeled tetravalent probes in high radiochemical yields. The aim of this study was thereby to demonstrate whether our design concept of metal coordination mediated multivalency could be extended to ^{99m}Tc-labeled tetravalent probes. For this purpose, here we examined the influence of the structure of isonitrile ligands on the formation of their corresponding ^{99m}Tc-labeled tetravalent probes.

Results and discussion

^{99m}Tc-labeling reaction of L_β and L_β'

Following the previous report,[18] we at first attempted synthesizing $[^{99m}Tc][Tc^{I}(CO)_2(L_\beta)_4]^+$ by reacting $[^{99m}Tc][Tc^{I}(CO)_3(OH_2)_3]^+$ with L_β at pH 8.0. Contrary to our expectation, however, multiple side products were generated at this slightly basic reaction condition (Fig. 4a). Since the formation of multiple side products was not observed in the previous report[18] where MIBI was used as a coordinating ligand, we speculated that the presence of RGD peptide might have caused some undesirable side reactions. To verify this speculation, we reacted $[^{99m}Tc][Tc^{I}(CO)_3(OH_2)_3]^+$ at pH 8.0 with CN-βAla-Gly-Gly-NH-Bn (Fig. 3, L_β'), where c(RGDfK) in L_β was replaced with benzylamine. However, as shown in Fig. 4b, the formation of multiple side products was again observed, suggesting that the side reaction observed here was not caused by the presence of RGD peptides but by other moieties in L_β.

Stabilities of ^{99m}Tc/Re-$[L_\beta']_3$ in acidic and basic solutions

To gain an insight into the mechanism of the side reaction, we evaluated the stabilities of ^{99m}Tc-$[L_\beta']_3$ and Re-$[L_\beta']_3$ at pH 8.0 (Fig. 5). Since technetium and rhenium share similar coordination chemistry due to their group homology, we employed non-radioactive rhenium analogues to characterize their tracer ^{99m}Tc counterparts. ^{99m}Tc-$[L_\beta']_3$ was prepared from a labeling

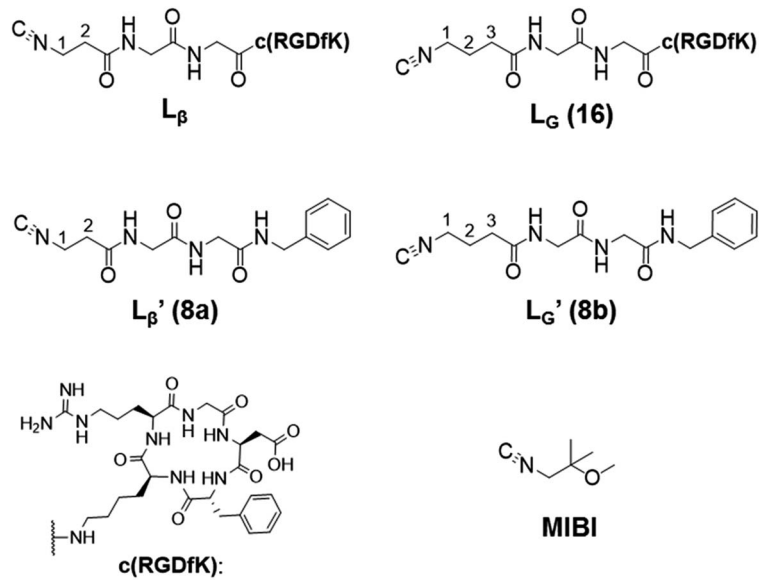

Fig. 3 The chemical structures of L_β, L_G, L_β', L_G', c(RGDfK), and MIBI.

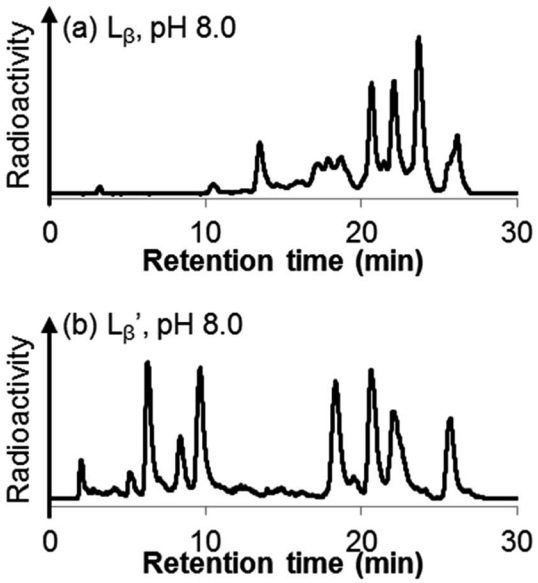

Fig. 4 HPLC analyses of ^{99m}Tc-labeling reactions under the conditions of (a) $[L_\beta] = 150$ μM, 110 °C for 20 min at pH 8.0 (system 11) and (b) $[L_\beta'] = 1$ mM, 100 °C for 30 min at pH 8.0 (system 6).

reaction at pH 6.0 and was purified by HPLC. ^{99m}Tc-$[L_\beta']_3$ was then dissolved in aqueous solution at pH 8.0 containing Re-$[L_\beta']_3$, and the solution was heated at 100 °C for 30 min. As shown in Fig. 5b, ^{99m}Tc-$[L_\beta']_3$ and Re-$[L_\beta']_3$ exhibited a similar decomposition pattern upon heating at pH 8.0, whereas they remained intact at pH 6.0 (Fig. S1†). These results indicate that the decomposition of ^{99m}Tc-$[L_\beta']_3$ under basic conditions primarily accounts for the generation of the multiple peaks observed in Fig. 4b.

We isolated compounds A, B and D (Fig. 5b) and determined their chemical structures by ^{1}H NMR, MS, and/or IR (Fig. 5c). The NMR spectrum of compound A showed coupling constants unique to geminal ($^2J_{HH} = 2$ Hz) and vicinal ($^3J_{HH} = 10$ and 17 Hz) couplings (Fig. S8b†), which proved the presence of an alkene structure. The IR spectrum of compound A (Fig. S8c†) also verified the presence of alkene (C=C, $\nu = 1647.88$ cm^{-1}) and excluded the presence of isonitrile, whose IR peak should appear at around 2150 cm^{-1}. On the other hand, compounds B and D showed MS spectra (Fig. S7a and S6a,† respectively) unique to rhenium isotopic patterns (the ratio of ^{185}Re/^{187}Re = 37/63). These results along with their m/z values indicated that compounds B and D had structures of $[Re^I(CO)_3(L_\beta')(CN)_2]^-$ and $[Re^I(CO)_3(L_\beta')_2(CN)]$, respectively (Fig. 5c).

The mechanism of the side reaction

The decomposition reaction of ^{99m}Tc/Re-$[L_\beta']_3$ has the following three characteristics: (1) one of the coordinated isonitrile ligands is eliminated from the Tc/Re-complex with leaving an isonitrile ion on the Tc/Re-complex, (2) the eliminated ligand loses the isonitrile group, and its terminal structure is converted to an alkene structure, (3) this reaction proceeds only at high hydroxide ion concentration. These features possess the characteristics of the "bimolecular elimination reaction".[19] We thereby hypothesized that the side reaction observed at basic conditions (Fig. 4) would also proceed *via* the following three simultaneous events: (1) the abstraction of the 2-proton in ^{99m}Tc-$[L_\beta']_3$ by a hydroxide ion, (2) the departure of $[^{99m}Tc][Tc^I(CO)_3(L_\beta')_2(CN)]$ from ^{99m}Tc-$[L_\beta']_3$, and (3) the formation of an alkene structure (Fig. 6).

Design and synthesis of L_G' and ^{99m}Tc-labeling of L_G'

According to the hypothesis proposed above, the high acidity of the 2-proton in L_β' (Fig. 6) would be essential for the side reaction to proceed. In addition, this high acidity of the 2-proton can be partly attributed to the electron withdrawing effect from the neighboring carbonyl group. We thereby newly

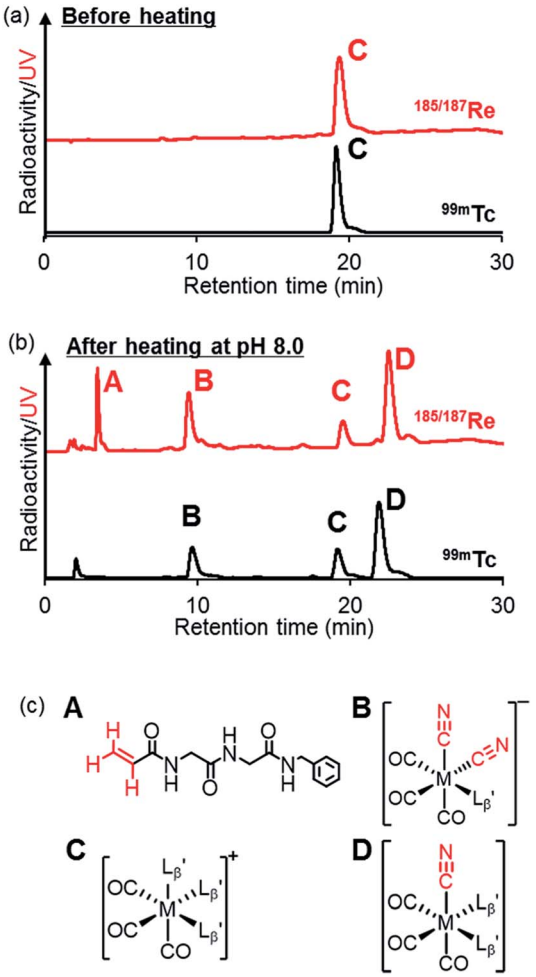

Fig. 5 The stability of M-$[L_\beta']_3$ (M = ^{99m}Tc and $^{185/187}$Re) in basic solution. HPLC analyses (system 6) of M-$[L_\beta']_3$ (a) before heating and (b) after heating at 100 °C for 30 min at pH 8.0. (c) The chemical structures of the products generated upon heating and the intact complex (M-$[L_\beta']_3$).

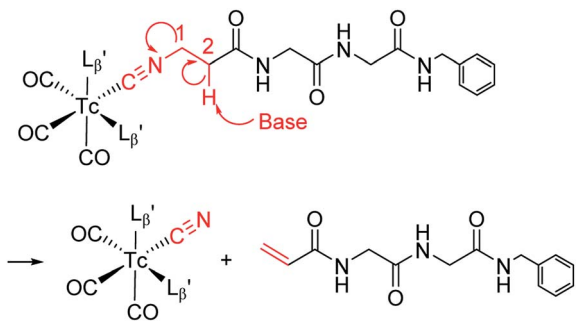

Fig. 6 A proposed reaction mechanism of the side reaction proceeding at basic conditions.

designed a γ-aminobutyric acid (GABA) based isonitrile ligand (L_G', Fig. 3). As the 2-proton in L_G' is no longer present next to the carbonyl group (Fig. 3), the 2-proton in L_G' would possess much lower acidity.

^{99m}Tc-labeling reactions of L_G' were performed in a procedure similar to that of L_β'. $[^{99m}Tc][Tc^I(CO)_3(OH_2)_3]^+$ was prepared as a labeling precursor, mixed with L_G' and heated at 100 °C for 30 min at pH 8.0. The HPLC analysis of this reaction solution is presented in Fig. 7c, which shows a completely different chromatographic profile from that in Fig. 4b. As shown in Fig. 7c, the ^{99m}Tc-labeling reaction of L_G' at pH 8.0 generated only two peaks, and the retention time of the major radioactivity peak was similar to that of $[Re^I(CO)_2(L_G')_4]^+$ (Re-$[L_G']_4$) characterized by ESI-MS and IR (Fig. 7b and c). These results supported the validity of our working hypothesis that the abstraction of the 2-proton by a base is the key step for the side reaction. We also identified the minor radioactivity peak as $[^{99m}Tc][Tc^I(CO)_3(L_G')_3]^+$ (^{99m}Tc-$[L_G']_3$) based on its similar HPLC retention time to that of $[Re^I(CO)_3(L_G')_3]^+$ (Re-$[L_G']_3$) (Fig. 7a and c).

A GABA-based isonitrile ligand with c(RGDfK) peptides

Based on the above findings, we subsequently designed and synthesized a GABA-based isonitrile ligand containing c(RGDfK) peptides (L_G, Fig. 3). The synthesis of L_G was accomplished by a condensation reaction of CN-GABA-TFP (**7b**) and H_2N-Gly-Gly-c(RGDfK) (**15**), followed by HPLC purification (Scheme S1†). Its corresponding rhenium complex, $[Re^I(CO)_2(L_G)_4]^+$ (Re-$[L_G]_4$), was also synthesized as a surrogate compound for its ^{99m}Tc counterpart.

As a result of preliminary evaluations on its ^{99m}Tc-labelling reactions, we established a reaction condition which reproducibly provides $[^{99m}Tc][Tc^I(CO)_2(L_G)_4]^+$ (^{99m}Tc-$[L_G]_4$) in over 90% radiochemical yields (Fig. 8). The ligand concentration required to provide ^{99m}Tc-$[L_G]_4$ (200 μM) was lower than that needed for ^{99m}Tc-$[L_\beta]_3$ (350 μM), which is advantageous to mitigate the competitive inhibition by unlabeled ligand *in vivo*.[9,20,21] Since isonitrile is more stable in basic solutions than in acidic ones,[22] the result that ^{99m}Tc-$[L_G]_4$ was prepared under lower ligand concentration could be attributed to the improved stability of the isonitrile moiety in L_G during the labeling reactions.

The stability of ^{99m}Tc-$[L_G]_4$ in an excess histidine solution and murine plasma was evaluated by TLC and HPLC. HPLC analyses were performed after removing plasma protein from the samples. The recovery rates of the radioactivity from plasma samples to supernatant solutions were 96.8 ± 0.4% ($n = 3$) upon addition of ethanol and protein precipitation. No decomposition of ^{99m}Tc-$[L_G]_4$ was observed at all even after 6 h incubation in both solutions (Table S1 and Fig. S2†). These results indicate that ^{99m}Tc-$[L_G]_4$ possesses stability sufficient for *in vivo* applications.

In vitro binding affinities of RGD derivatives

To examine the differences in integrin $\alpha_v\beta_3$ binding affinities between monovalent and tetravalent RGD peptides, we calculated the IC_{50} values of L_G and Re-$[L_G]_4$ in a competitive binding experiment using $[^{125}I]$I-c(RGDyV) and U87MG cell as a competed radioligand and an integrin $\alpha_v\beta_3$ positive cell line, respectively. We included c(RGDyV) into the study as an internal standard. As shown in Table 1 and Fig. S3†, Re-$[L_G]_4$ showed

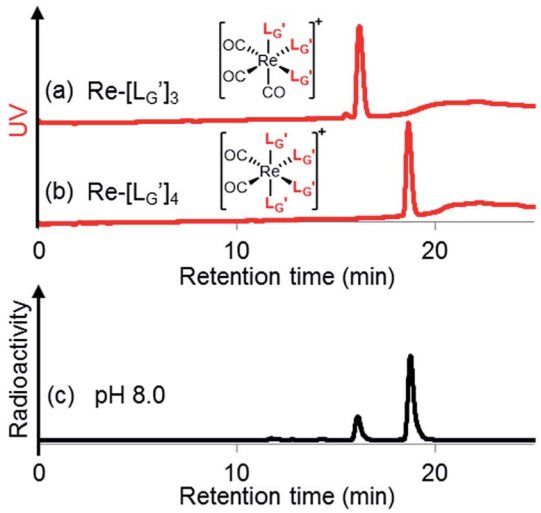

Fig. 7 HPLC analyses (system 7) of (a) Re-[L_G']$_3$ and (b) Re-[L_G']$_4$. (c) An HPLC analysis (system 7) of a ^{99m}Tc-labeling reaction of L_G' under the condition of L_G' = 1 mM, 100 °C for 30 min at pH 8.0.

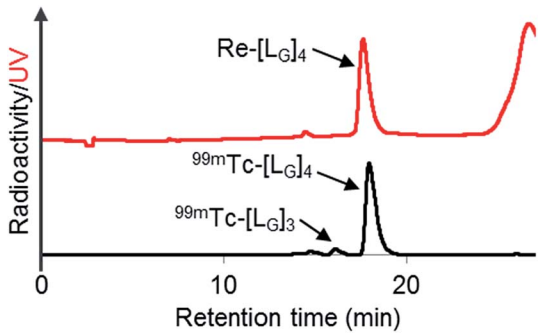

Fig. 8 HPLC analyses (system 9) of Re-[L_G]$_4$ and a ^{99m}Tc-labeling reaction performed under the condition of [L_G] = 200 μM, 85 °C for 1 h, and 37.5 mM P.B. (pH 8.0).

Table 1 The IC_{50} values of each compound

Compound	IC_{50}, nM	95% C.I.[a]
L_G	107	90.2–126
Re-[L_G]$_4$	2.59	1.90–3.54
c(RGDyV)	34.8	27.5–44.0

[a] C.I. = confidential interval.

much lower IC_{50} value than those of L_G and c(RGDyV), indicating that the metal complex has gained enhanced binding affinity due to the multivalent effect. This superior binding affinity is essential for ^{99m}Tc-[L_G]$_4$ to achieve high *in vivo* target uptake when injected into subjects without post-labeling purification.

In vivo study of ^{99m}Tc-[L_G]$_4$

We evaluated the biodistribution of ^{99m}Tc-[L_G]$_4$ in U87MG-bearing nude mice at 1 h post injection, and these results are summarized in Table 2. There were three different samples tested in this study: (1) HPLC-purified ^{99m}Tc-[L_G]$_4$ (without the unlabeled ligand (L_G)), (2) unpurified ^{99m}Tc-[L_G]$_4$ (containing 5 nmol of L_G) and (3) HPLC-purified ^{99m}Tc-[L_G]$_4$ with 5 nmol of Re-[L_G]$_4$. The second sample represent our chemical design where a ^{99m}Tc-labeled multivalent RGD probe prepared from a monovalent ligand is injected into subjects without post-labeling purification (Fig. 1b), whereas the third sample imitates a conventional design where a ^{99m}Tc-labeled tetravalent RGD probe prepared from a ligand already possessing tetravalent RGD is injected into subjects without postlabeling purification (Fig. 1a). Though the tumor uptake of ^{99m}Tc-[L_G]$_4$ was slightly impaired by the presence of 5 nmol of L_G in the injectate (5.00 ± 0.84% ID g^{-1} *vs.* 3.08 ± 0.43% ID g^{-1}), its tumor uptake value was significantly higher than that of the conventional design (3.08 ± 0.43% ID g^{-1} *vs.* 1.81 ± 0.14% ID g^{-1}).

The tumor to blood ratio of un-purified ^{99m}Tc-[L_G]$_4$ was not higher than that of purified ^{99m}Tc-[L_G]$_4$ + Re-[L_G]$_4$. This is attributed to the higher blood radioactivity level of unpurified ^{99m}Tc-[L_G]$_4$ (0.58 ± 0.39% ID g^{-1}) than that of purified ^{99m}Tc-[L_G]$_4$ + Re-[L_G]$_4$ (0.21 ± 0.04% ID g^{-1}). Though further study would be needed to elucidate the cause of the higher blood radioactivity level, we are considering the possibility that the difference in the normal tissue uptakes (Table 2) affected the blood clearance of ^{99m}Tc-[L_G]$_4$, especially in the elimination phase. Because blood clearance in the elimination phase can be affected by redistribution from normal tissues, the higher normal tissue uptakes could cause higher blood radioactivity level in the elimination phase.

Lastly, we performed a SPECT/CT imaging study using unpurified ^{99m}Tc-[L_G]$_4$ containing 5 nmol of L_G. A representative SPECT/CT image is shown in Fig. 9, which clearly visualized U87MG tumor despite the presence of excess unlabeled ligand in the injectate, owing to the high tumor uptake of ^{99m}Tc-[L_G]$_4$. These results again demonstrated the utility of our design concept for achieving high *in vivo* target uptake of ^{99m}Tc-labeled probes without tedious post-labeling purification.

Conclusion

In this study, we have found a way to prepare a ^{99m}Tc-labeled tetravalent RGD probe upon isonitrile ligands coordination to $^{99m}Tc^{I}$ in the molar ratio of 4 to 1. Our initial attempts reacting a βAla-based isonitrile ligand (L_β) with $[^{99m}Tc][Tc(CO)_3]^+$ core at pH 8.0 failed to provide $[^{99m}Tc][Tc(CO)_2(L_\beta)_4]^+$ due to the bimolecular elimination reaction. GABA-based isonitrile ligands (L_G and L_G'), on the other hand, avoided the side reaction and provided ^{99m}Tc-labeled tetravalent probes from reactions at basic conditions. In the SPECT/CT study, ^{99m}Tc-[L_G]$_4$ clearly visualized integrin $\alpha_v\beta_3$ positive tumor without tedious post-labeling purification to remove its excess unlabeled ligand. These results clearly indicate that the metal coordination-mediated synthesis of ^{99m}Tc-labeled bivalent and trivalent probes has been successfully extended to that of tetravalent ones, which would lead to a wider range of choices for designing novel ^{99m}Tc-labeled multivalent probes of high *in vivo* target uptake. In addition, because ^{99m}Tc-hexakis-isonitriles such as

Table 2 Biodistribution at 1 h postinjection in U87MG-bearing mice[a]

Tissue	Purified ^{99m}Tc-[L_G]$_4$ (L_G = 0 nmol)	Un-purified ^{99m}Tc-[L_G]$_4$ (L_G = 5 nmol)	Purified ^{99m}Tc-[L_G]$_4$ + Re-[L_G]$_4$ (Re-[L_G]$_4$ = 5 nmol)
Blood	0.26 ± 0.04	0.58 ± 0.39	0.21 ± 0.04
Liver	1.85 ± 0.23	1.29 ± 0.14	0.95 ± 0.14
Spleen	2.16 ± 0.31	1.29 ± 0.12	0.95 ± 0.09
Kidney	13.05 ± 0.87	13.12 ± 1.87	12.28 ± 1.14
Pancreas	0.93 ± 0.07	0.46 ± 0.06	0.27 ± 0.05
Heart	1.10 ± 0.13	0.52 ± 0.05	0.36 ± 0.07
Lung	2.25 ± 0.47	1.60 ± 0.11	0.84 ± 0.25
Stomach	4.57 ± 2.43	4.21 ± 2.01	2.36 ± 0.83
Intestine	4.01 ± 0.89	3.34 ± 1.06	1.99 ± 0.65
Muscle	0.74 ± 0.17	0.44 ± 0.12	0.26 ± 0.23
Tumor[b]	5.00 ± 0.84*	3.08 ± 0.43	1.81 ± 0.14*
T/Blood	19.0 ± 2.31	6.15 ± 3.03	8.81 ± 1.48
T/Liver	2.72 ± 0.49	2.35 ± 0.40	1.93 ± 0.22
T/Muscle	7.10 ± 2.04	7.19 ± 2.12	9.60 ± 4.11

[a] The results were expressed as percent injected dose per gram (% ID g^{-1}) ± SD (n = 5 or 6). [b] Statistical analysis was performed using one-way analysis of variance followed by Tukey's multiple-comparison test (* different from "un-purified ^{99m}Tc-[L_G]$_4$ (L_G = 5 nmol)", $p < 0.01$).

Fig. 9 A SPECT/CT image of a U87MG tumor-bearing male nude mouse over 30–94 min post i.v. injection of 3.7 MBq of ^{99m}Tc-[L_G]$_4$ containing 5 nmol of L_G. Red circle indicates the U87MG tumor.

[^{99m}Tc][Tc(MIBI)$_6$]$^+$ also possess very high *in vivo* stability, we are currently working to apply our metal coordination mediated multivalency concept to hexavalent ones, and are going to report the results in the near future elsewhere.

Experimental section

General

[$^{185/187}$Re(CO)$_3$(OH$_2$)$_3$]Br (**19**),[23] Boc-Gly-Gly-OH (**1**),[10] CN-βAla-TFP (**7a**),[10] CN-βAla-Gly-Gly-c(RGDfK) (L_β)[10] and H_2N-Gly-Gly-c(RGDfK)·CF_3CO_2H (**15**)[10] were synthesized according to the previous reports. Technetium-99m as Na^{99m}TcO$_4$ was eluted in saline solution on daily basis from a ^{99}Mo/^{99m}Tc generator (FUJIFILM RI Pharma Co., Ltd., Tokyo, Japan). All other reagents were purchased from Wako Pure Chemical Industries, Ltd. (Tokyo, Japan) and were used without further purification. Mass spectrometry was carried out using a JMS-T100LP (JEOL Ltd., Tokyo, Japan) or an Agilent 6130 Series Quadrupole LC/MS spectrometer (Agilent technologies, Tokyo). ^{1}H NMR/^{13}C NMR spectra was recorded on a JEOL ECS-400 (400 MHz/100 MHz, respectively) spectrometer (JEOL Ltd, Tokyo). Infrared (IR) spectra were recorded on a FT/IR-4700 (Jasco Co., Tokyo, Japan).

Boc-Gly-Gly-NH-Bn (2)

Boc-Gly-Gly-OH (**1**) (180 mg, 0.775 mmol) and benzylamine (77 μL, 0.705 mmol) were dissolved in dichloromethane (4 mL). To this stirred mixture was added 1-ethyl-3-(3-dimethylaminopropyl)carbodiimide hydrochloride (EDC HCl, 270 mg, 1.41 mmol), and the mixture was stirred at room temperature for 1 h. The solvent was removed *in vacuo* and the residue was dissolved in chloroform (15 mL) and washed with 5% citric acid (10 mL) and 5% $NaHCO_3$ (10 mL). The organic layer was then dried over magnesium sulfate. After removing magnesium sulfate by filter, the organic solvent was removed *in vacuo* to afford the compound **2** as a white solid (189 mg, 76%). ^{1}H NMR (400 MHz, DMSO-d_6): δ 1.37 (s, 9H, *t*Bu), 3.57 (d, 2H, Hα_{Gly}), 3.74 (d, 2H, Hα_{Gly}), 4.29 (d, 2H, CH_2-phenyl), 7.05 (t, 1H, N*H*), 7.21–7.33 (m, 5H, H_{arom}), 8.11 (t, 1H, N*H*), 8.28 (t, 1H, N*H*). ^{13}C NMR (100 MHz, DMSO-d_6): δ 28.16 (C(*C*H$_3$)$_3$), 41.96 (Cα_{Gly}), 42.07 (*C*H$_2$-phenyl), 43.42 (Cα_{Gly}), 78.16 (*C*(CH$_3$)$_3$), 126.73 (C$_{arom}$), 127.10 (C$_{arom}$), 128.22 (C$_{arom}$), 139.24 (C$_{arom}$), 155.91 (*C*O), 168.79 (*C*O), 169.74 (*C*O). ESI-MS, m/z: 322.18 [M + H]$^+$, found 322.24.

H_2N-Gly-Gly-NH-Bn·CF_3CO_2H (3)

The compound **2** (104 mg, 0.324 mmol) was dissolved in trifluoroacetic acid (TFA, 2.5 mL) and stirred at room temperature for 1 h. After removing TFA *in vacuo*, the compound **3** was successively used in the following condensation reactions without further purification.

4-Formylaminobutanoic acid (5b)

4-Aminobutanoic acid (2.00 g, 19.4 mmol) was dissolved in formic acid/acetic anhydrate (20 mL/15 mL) and stirred at 95 °C under N_2 atmosphere for 30 min. After the solvent was evaporated *in vacuo*, the residue was washed with diethyl ether to afford the compound **5b** as a white solid (1.00 g, 39%). ^{1}H NMR (400 MHz, DMSO-d_6): δ 1.62 (m, 2H, $CH_2CH_2CH_2$), 2.22 (t, 2H, CH_2CO), 3.08 (q, 2H, $NHCH_2$), 7.99 (s, 1H, formylamino), 8.02 (s, 1H, N*H*). ESI-MS, *m*/*z*: 130.05 $[M - H]^-$, found 130.09.

2,3,5,6-Tetrafluorophenyl 4-formylaminobutanoate (6b)

The compound **5b** (525 mg, 4.00 mmol) and 2,3,5,6-tetrafluoro phenol (TFP, 797 mg, 4.80 mmol) were dissolved in chloroform (8 mL). To this stirred mixture was added EDC HCl (1.53 g, 8.00 mmol), and the mixture was stirred at room temperature for 2 hours. The solvent was removed *in vacuo* and purified with silica gel column chromatography (hexane/ethyl acetate = 1/1) to afford the compound **6b** as a white powder (929 mg, 83%). ^{1}H NMR (400 MHz, DMSO-d_6): δ 1.81 (m, 2H, $CH_2CH_2CH_2$), 2.81 (t, 2H, CH_2CO), 3.18 (q, 2H, $NHCH_2$), 7.95 (m, 1H, H_{arom}), 8.03 (s, 1H, formylamino), 8.11 (s, 1H, N*H*). ESI-MS, *m*/*z*: 302.04 $[M + Na]^+$, found 301.97.

2,3,5,6-Tetrafluorophenyl 4-isocyanobutanoate (CN-GABA-TFP) (7b)

The compound **6b** (717 mg, 2.57 mmol) and Burgess reagent[24] (918 mg, 3.85 mmol) were dissolved in dichloromethane (24 mL) and stirred at 50 °C for 30 minutes. After removing the solvent *in vacuo*, the residue was purified with silica gel chromatography (hexane/ethyl acetate = 10/1) to afford the compound **7b** as a dark yellow oil (404 mg, 60%). ^{1}H NMR (400 MHz, $CDCl_3$): δ 2.16 (br, 2H, $CH_2CH_2CH_2$), 2.91 (t, 2H, CH_2CO), 3.59 (m, 2H, NCH_2), 7.02 (m, 1H, H_{arom}). IR (ATR, ν/cm^{-1}): 2149.28 (s, C≡N).

CN-βAla-Gly-Gly-NH-Bn (L_β') (8a)

CN-βAla-TFP (**7a**) was synthesized as previously reported.[10] To a solution of the compound **7a** (120 mg, 0.486 mmol) and H_2N-Gly-Gly-NH-Bn·CF_3CO_2H (**3**) (108.6 mg, 0.324 mmol) in *N*,*N*-dimethylformamide (DMF, 2 mL) was added $NaHCO_3$ (40.8 mg, 0.486 mmol). The mixture was stirred at room temperature for 1 h. After removing $NaHCO_3$ by filtration, the solvent was removed *in vacuo* and the crude compound was purified with silica gel column chromatography (chloroform/methanol = 20/1) to afford the compound **8a** as a white solid (70 mg, 72%). ^{1}H NMR (400 MHz, DMSO-d_6): δ 2.56 (br, 2H, CH_2CH_2CO), 3.64 (br, 2H, CH_2CH_2CO), 3.74 (d, 2H, $H\alpha_{Gly}$), 3.77 (d, 2H, $H\alpha_{Gly}$), 4.29 (d, 2H, CH_2-phenyl), 7.21–7.33 (m, 5H, phenyl), 8.23 (t, 1H, N*H*), 8.29 (t, 1H, N*H*), 8.37 (t, 1H, N*H*). ^{13}C NMR (100 MHz, DMSO-d_6): δ 34.47 (CH_2CH_2CO), 37.47 (t, CH_2CH_2CO), 41.97 ($C\alpha_{Gly}$), 42.07 ($C\alpha_{Gly}$), 42.23 (CH_2-phenyl), 126.76 (C_{arom}), 127.17 (C_{arom}), 128.25 (C_{arom}), 139.32 (C_{arom}), 155.73 (t, *C*N), 168.78 (*C*O), 169.15 (2C, *C*O). ESI-MS, *m*/*z*: 325.13 $[M + Na]^+$, found 325.19. IR (ATR, ν/cm^{-1}): 2150.24 (s, C≡N).

CN-GABA-Gly-Gly-NH-Bn (L_G') (8b)

To a solution of CN-GABA-TFP (**7b**) (106.8 mg, 0.409 mmol) and H_2N-Gly-Gly-NH-Bn·CF_3CO_2H (**3**) (100.2 mg, 0.299 mmol) in DMF (2 mL) was added $NaHCO_3$ (75.2 mg, 0.895 mmol). The mixture was stirred at room temperature for 6 h. After removing $NaHCO_3$ by filtration, the solvent was removed *in vacuo* and the crude product was purified with silica gel column chromatography (chloroform/methanol = 20/1) to afford the compound **8b** as a white solid (60 mg, 63%). ^{1}H NMR (400 MHz, DMSO-d_6): δ 1.79 (m, 2H, $CH_2CH_2CH_2$), 2.27 (t, 2H, $CH_2CH_2CH_2$), 3.50 (m. 2H, $CNCH_2$), 3.72 (d, 2H, $H\alpha_{Gly}$), 3.74 (d, 2H, $H\alpha_{Gly}$), 4.28 (d, 2H, CH_2-phenyl), 7.21–7.33 (m, 5H, H_{arom}), 8.23 (t, 1H, N*H*), 8.28–8.32 (m, 2H, N*H*). ESI-MS, *m*/*z*: 339.14 $[M + Na]^+$, found 339.16. IR (ATR, ν/cm^{-1}): 2147.35 (s, C≡N).

$[Re^I(CO)_3(L_\beta')_3]CF_3CO_2$ (Re-$[L_\beta']_3$) (9)

$[Re^I(CO)_3(OH_2)_3]Br$ (**19**) (9.7 mg, 0.024 mmol) and L_β' (**8a**) (65 mg, 0.215 mmol) were dissolved in 0.1 M acetate buffer (pH 6.0, 21.5 mL). After heating at 100 °C for 3 h, the crude was purified by preparative HPLC using system 1 and lyophilized to afford the compound **9** as a white powder (30 mg, 97%). ^{1}H NMR (400 MHz, DMSO-d_6): δ 2.70 (t, 2H, CH_2CH_2CO), 3.76 (d, 2H, $H\alpha_{Gly}$), 3.81 (d, 2H, $H\alpha_{Gly}$), 4.09 (t, 2H, CH_2CH_2CO), 4.28 (d, 2H, CH_2-phenyl), 7.21–7.33 (m, 5H, H_{arom}), 8.27 (t, 1H, N*H*), 8.36 (t, 1H, N*H*), 8.43 (t, 1H, N*H*). ^{13}C NMR (100 MHz, DMSO-d_6): δ 33.89 (CH_2CH_2CO), 41.06 (CH_2CH_2CO), 42.02, 42.08, ($C\alpha_{Gly}$, CH_2-phenyl), 126.79 (C_{arom}), 127.18 (C_{arom}), 128.26 (C_{arom}), 139.31 (C_{arom}), 158.24 (q, *C*N), 168.80 (*C*O), 168.96 (*C*O), 169.10 (*C*O), 182.71 (Re*C*O). ESI-MS, *m*/*z*: 1177.35 $[M]^+$, found 1177.56. IR (ATR, ν/cm^{-1}): 2244.74 (w, C≡N), 2212.92 (m, C≡N), 2057.67, 1990.18 (s, C≡O).

$[Re^I(CO)_3(L_G')_3]CF_3CO_2$ (Re-$[L_G']_3$) (10)

$[Re^I(CO)_3(OH_2)_3]Br$ (**19**) (2.6 mg, 6.4 μmol) and L_G' (**8b**) (20 mg, 63.2 μmol) were dissolved in 0.1 M phosphate buffer (P.B., pH 7.0, 6.32 mL). After heating at 100 °C for 3 h, the crude was purified by preparative HPLC using system 3 and lyophilized to afford the compound **10** as a white powder (8.9 mg, quant.). ^{1}H NMR (400 MHz, DMSO-d_6): δ 1.93 (m, 2H, $CH_2CH_2CH_2$), 2.29 (t, 2H, $CH_2CH_2CH_2$), 3.75 (d, 4H, $H\alpha_{Gly}$), 3.98 (t, 2H, $CNCH_2$), 4.28 (d, 2H, CH_2-phenyl), 7.10–7.33 (m, 5H, H_{arom}), 8.23 (t, 1H, N*H*), 8.29 (t, 1H, N*H*), 8.34 (t, 1H, N*H*). ESI-MS, *m*/*z*: 1219.40 $[M]^+$, found 1219.47. IR (ATR, ν/cm^{-1}): 2238.95 (w, C≡N), 2208.09 (m, C≡N), 2053.82, 1981.50 (s, C≡O).

$[Re(CO)_2(L_G')_4]CF_3CO_2$ (Re-$[L_G']_4$) (11)

Re-$[L_G']_3$ (**10**) (3.6 mg, 0.0027 mmol) and L_G' (**8b**) (4.7 mg, 0.0149 mmol) were dissolved in 0.1 M P.B. (pH 8.0, 1.47 mL). The mixture was heated at 100 °C for 6 h, after which time additional L_G' (**8b**) (4.7 mg, 0.0149 mmol) was added. After heating at 100 °C for another 6 h, the crude product was purified by preparative HPLC using system 3 and lyophilized to afford the compound **11** as a white powder (0.4 mg, 10%). ESI-MS, *m*/*z*: 1507.56 $[M]^+$, found 1507.65. IR (ATR, ν/cm^{-1}): 2228.34 (w, C≡N), 2160.85 (s, C≡N), 1996.93, 1953.54 (s, C≡O).

$[^{99m}Tc][Tc^{I}(CO)_3(OH_2)_3]^+$

$[^{99m}Tc][Tc^{I}(CO)_3(OH_2)_3]^+$ was prepared according to a reported method[25] with slight modifications. Briefly, a kit containing 0.285 mg sodium tetraborate decahydrate ($Na_2B_4O_7\cdot 10H_2O$), 0.715 mg sodium carbonate (Na_2CO_3), 1 mg sodium(+)-tartrate dihydrate ($C_4H_4Na_2O_6\cdot 2H_2O$), and 0.45 mg sodium boranocarbonate [$Na_2(H_3BCO_2)$] was purged with N_2 atmosphere before adding 300 μL [^{99m}Tc]TcO_4^- (~333 MBq) to a sealed vial. After the mixture was heated for 14 min at 100 °C, the vial was allowed to stand at room temperature for 3 min. The pH of the solution was then adjusted to 6, 7, or 8 with 1 M AcOH. Ten min after the neutralization, $AgNO_3$ (7.1 mg, 0.042 mmol) was added to the solution to precipitate out Cl^- as AgCl. After filtering the solution through 0.45 μm Cosmonice Filter W (NACALAI TESQUE, Inc., Kyoto), the solution was used for labeling reactions with L_β and L_G. For the reactions with L_β' and L_G', 1N HCl was used for neutralization and $[^{99m}Tc][Tc^{I}(CO)_3(OH_2)_3]^+$ solution was used without the removal of Cl^-.

^{99m}Tc-labeling reaction of L_β

A 5 μL of freshly prepared $[^{99m}Tc][Tc^{I}(CO)_3(OH_2)_3]^+$ (~5.55 MBq) was added to a vial containing 95 μL of L_β solution (0.1 M P.B., pH 8.0) to reach the final ligand concentration of 150 μM. The mixture was heated at 110 °C for 20 min under N_2 atmosphere in a heating block. The reaction solution was analyzed by HPLC using system 11.

^{99m}Tc-labeling reaction of L_β'

A 20 μL solution of freshly prepared $[^{99m}Tc][Tc^{I}(CO)_3(OH_2)_3]^+$ (~22.2 MBq) was added to a vial containing 380 μL of L_β' solution (0.1 M P.B., pH 6.0 or 8.0) to reach the final ligand concentration of 1 mM. The mixtures were heated at 100 °C for 30 min under N_2 atmosphere in a heating block. The reaction solutions were analyzed by HPLC using system 6.

Stability of ^{99m}Tc/Re-$[L_\beta']_3$ in acidic and basic solutions

^{99m}Tc-$[L_\beta']_3$ was prepared by the reaction at pH 6.0 which was described above and purified by HPLC (system 6). The eluent of the objective fraction was evaporated *in vacuo* and the residue was dissolved in 0.1 M P.B. (pH 6.0 or 8.0) containing 40 nmol of Re-$[L_\beta']_3$ to prepare 111 kBq ^{99m}Tc-$[L_\beta']_3$/40 nmol Re-$[L_\beta']_3$/100 μL sample solutions. The sample of pH 6.0 was analyzed by HPLC (system 6) before heating. Both solutions were then heated at 100 °C for 30 min in a heating block and analyzed by HPLC (system 6) after heating.

Characterization of three peaks generated upon heating Re-$[L_\beta']_3$

Re-$[L_\beta']_3$ (**9**) was prepared by the method described above. Twenty nine mg of Re-$[L_\beta']_3$ (0.225 mmol) was dissolved in 5 mL of 0.1 M P.B. (pH 8.0) and the mixture was heated at 100 °C for 5 h. The crude product was purified by preparative HPLC using system 2 to afford the compound **12** (1.4 mg, 23% calculated from the Re-complex) as a white solid, the compound **14** (1.8 mg, 13%) as a purple oil and the compound **13** (6.1 mg, 30%) as an orange solid. The spectrum data of the compound **12**, **13** and **14** are shown down below.

The eliminated ligand (compound A in Fig. 5b) (12)

^{1}H NMR (400 MHz, DMSO-d_6): δ 3.75 (d, 2H, Hα_{Gly}), 3.83 (d, 2H, Hα_{Gly}), 4.28 (d, 2H, CH_2-phenyl), 5.61 (dd, 1H, J = 2, 10 Hz, H_{alkene}), 6.08 (dd, 1H, J = 2, 17 Hz, H_{alkene}), 6.31 (dd, 1H, J = 10, 17 Hz, H_{alkene}), 7.21–7.33 (m, 5H, H_{arom}), 8.27 (t, 1H, N*H*), 8.34 (t, 1H, N*H*), 8.44 (t, 1H, N*H*). ESI-MS, *m*/*z*: 298.12 $[M + Na]^+$, found 298.10. IR (ATR, ν/cm^{-1}): 1647.88 (s, C=C).

$[Re(CO)_3(L_\beta')_2(CN)]$ (compound D in Fig. 5b) (13)

^{1}H NMR (400 MHz, DMSO-d_6): δ 2.69 (t, 2H, CH_2CH_2CO), 3.75 (d, 2H, Hα_{Gly}), 3.80 (d, 2H, Hα_{Gly}), 4.07 (t, 2H, CH_2CH_2CO), 4.28 (d, 2H, CH_2-phenyl), 7.21−7.33 (m, 5H, H_{arom}), 8.26 (t, 1H, N*H*), 8.30 (t, 1H, N*H*), 8.44 (t, 1H, N*H*). ESI-MS, *m*/*z*: 924.21 $[M + Na]^+$, found 924.38.

$[Re(CO)_3(L_\beta')(CN)_2]^-$ (compound B in Fig. 5b) (14)

ESI-MS, *m*/*z*: 627.10 $[M + 2H]^+$, found 627.22.

^{99m}Tc-labeling reaction of L_G'

A 20 μL solution of freshly prepared $[^{99m}Tc][Tc^{I}(CO)_3(OH_2)_3]^+$ (~22.2 MBq) was added to a vial containing 380 μL of L_G' solution (0.1 M P.B., pH 8.0) to reach the final ligand concentration of 1 mM. The mixtures were heated at 100 °C for 30 min under N_2 atmosphere in a heating block. The reaction solutions were analyzed by HPLC using system 7.

CN-GABA-Gly-Gly-c(RGDfK) (L_G) (16)

To a solution of the compound **15** (13.8 mg, 16.6 μmol) and *N*,*N*-diisopropylethylamine (4.9 μL, 28.8 μmol) in DMF (180 μL) was added the compound **7b** (4.0 mg, 16 μmol). The reaction mixture was stirred at room temperature for 1 h, after which time diethyl ether was added to the solution to form precipitate. The precipitate was collected and purified with preparative HPLC using system 4, and lyophilized to afford the compound **16** as a white powder (7.0 mg, 52%). ESI-MS, *m*/*z*: 813.40 $[M + H]^+$, found 813.49.

$[Re^{I}(CO)_3(L_G)_3]CF_3CO_2$ (Re-$[L_G]_3$) (17) and $[Re^{I}(CO)_2(L_G)_4]CF_3CO_2$ (Re-$[L_G]_4$) (18)

L_G (**16**) (6.0 mg, 7.4 μmol) and $[Re^{I}(CO)_3(OH_2)_3]Br$ (**19**) (0.3 mg, 0.7 μmol) were dissolved in 50 mM P.B. (pH 8.0, 720 μL). The mixture was heated at 110 °C for 2 h, after which time additional L_G (1.5 mg, 1.9 μmol) was added to the solution. After heating at 110 °C for another 2 h, the crude was purified with preparative HPLC using system 5 and lyophilized to afford the compounds **17** and **18** as white powders (0.5 mg and 25% for the compound **17**, and 0.2 mg and 8% for the compound **18**). ESI-MS (**17**), *m*/*z*: 1355.06 $[M + H]^{2+}$, found 1355.26. ESI-MS (**18**), *m*/*z*: 874.13 $[M + 3H]^{4+}$, found 874.4.

^{99m}Tc-labeling reaction of L_G

L_G (**16**) (20 nmol) was dissolved in 75 μL of 50 mM P.B. at pH 8.0. A 25 μL solution of freshly prepared $[^{99m}Tc][Tc^{I}(CO)_3(OH_2)_3]^+$ (~27.8 MBq) was added to this L_G solution, followed by heating at 85 °C for 1 h under N_2 atmosphere. The resulting solution was analyzed by HPLC using system 9.

Stability assessment

The unlabeled ligand in ^{99m}Tc-$[L_G]_4$ was removed by HPLC using system 9. The radioactive peak was collected and the solvent was removed *in vacuo*. The residue was reconstituted in 0.001% v/v TritonX-100 in D-PBS(−), and 10 μL of the ^{99m}Tc-$[L_G]_4$ solution was mixed with 190 μL of histidine solution to reach the final histidine concentration of 10 mM. Similarly 10 μL of the ^{99m}Tc-$[L_G]_4$ solution was mixed with 190 μL of freshly prepared murine plasma. After incubation at 37 °C for 1 and 6 h, 1 μL of aliquots were drawn and analyzed with radio-TLC ($n = 3$) (Silica gel 60 F_{254}, Merck Ltd., Tokyo) developed with MeOH : 10% w/w $AcONH_4$ in water = 1 : 1. For HPLC analysis of the histidine sample, the incubation solution was directly analyzed by HPLC using system 9. For HPLC analysis of the plasma sample, 200 μL of EtOH was added to 100 μL of the plasma sample to precipitate the proteins. The sample was centrifuged at 15 000*g* for 5 min at 4 °C. The supernatant was collected and, the pellet was washed with 300 μL of 66% v/v EtOH in D-PBS(−) and centrifuged. This washing step was repeated twice. The supernatants of both centrifugation steps were combined and analyzed by HPLC using system 9. The recovery rate of radioactivity from the plasma sample was determined by following equation, (the radioactivity of the supernatant)/(the original radioactivity of the plasma sample) × 100 ($n = 3$). The radioactivity was determined using an autowell γ counter (WIZARD 1480, PerkinElmer Japan Co., Ltd., Yokohama, Japan).

Binding affinity to integrin $\alpha_v\beta_3$

U87MG human glioma cells were grown in Dulbecco's Modified Eagle Medium (Sigma-Aldrich Japan K.K., Tokyo) supplemented with 10% v/v fetal bovine serum (Nippon Biosupply Center, Tokyo), and 1% v/v penicillin–streptomycin (10 000 unit–10 mg mL^{-1}, Sigma-Aldrich Japan K.K.) at 37 °C in humidified atmosphere containing 5% CO_2. Multiscreen DV filter plates (Merck Millipore, MA) were seeded with 2×10^5 cells in the binding buffer (20 mM Tris, 150 mM NaCl, 2 mM $CaCl_2$, 1 mM $MgCl_2$, 1 mM $MnCl_2$, 0.1% BSA, pH 7.4) and the mixtures were incubated at 37 °C with [^{125}I]I-c(RGDyV) in the presence of increasing concentrations of c(RGDyV), L_G, Re-$[L_G]_3$, or Re-$[L_G]_4$. The total incubation volume was adjusted to 200 μL. After incubation for 1 h at 37 °C, the plates were filtered, and washed twice with 200 μL of the ice cold binding buffer. The polyvinylidene fluoride (PVDF) filters were collected and the radioactivity was determined using an autowell γ counter. The IC_{50} values were calculated by fitting the data by nonlinear regression using GraphPad Prism (GraphPad Software, Inc., San Diego, CA). All the binding experiments were carried out with quadruplet samples.

Animal model

All animal procedures were performed in accordance with the institutional guidelines approved by the Chiba University Animal Care Committee and experiments were approved by the Chiba University Animal Care Committee. BALBc nu/nu male mice (Japan SLC, Inc., Shizuoka, Japan) of 6 week-old were xenografted by subcutaneous injection of U87MG human glioblastoma cells (5×10^6 cells per 50 μL of culture medium) into their right hind legs. The mice were subjected to biodistribution studies as well as SPECT/CT imaging studies when the tumor weight reached 0.1–0.5 g.

Biodistribution

Male nude mice bearing tumor xenografts of U87MG were injected *via* the tail vein with 100 μL (11.1 kBq) of ^{99m}Tc-$[L_G]_4$ (L_G = 0 nmol), ^{99m}Tc-$[L_G]_4$ ($L_G = 5$ nmol) or ^{99m}Tc-$[L_G]_4$ (Re-$[L_G]_4 = 5$ nmol). ^{99m}Tc-$[L_G]_4$ (L_G = 0 nmol) was prepared by diluting an HPLC-purified ^{99m}Tc-$[L_G]_4$ solution with D-PBS (−). ^{99m}Tc-$[L_G]_4$ (Re-$[L_G]_4$ = 5 nmol) was prepared by adding Re-$[L_G]_4$ to an HPLC-purified ^{99m}Tc-$[L_G]_4$ solution. Un-purified ^{99m}Tc-$[L_G]_4$ solution was used for ^{99m}Tc-$[L_G]_4$ (L_G = 5 nmol). The animals were sacrificed and dissected at 1 h after administration. The tissues of interest were removed and weighed, and the radioactivity was determined with an autowell gamma counter. The results are presented as the percentage injected dose per gram (% ID g^{-1}) or percentage injected dose per tissue (% ID). Values were expressed as mean ± SD for a group of 5 or 6 animals.

Small animal SPECT/CT imaging study

SPECT images were acquired over 30–94 min after intravenous administration of ^{99m}Tc-$[L_G]_4$ (100 μL, 3.7 MBq, $L_G = 5$ nmol) to male BALBc nu/nu mice bearing U87MG xenografts *via* the tail vein. CT scans were performed before SPECT scans for anatomic reference. The mice were anaesthetized with 1–2% (v/v) isoflurane (DS Pharma Animal Health, Osaka, Japan) and positioned on the animal bed where anesthesia was continuously delivered *via* a nose cone system. SPECT imaging and X-ray CT imaging were performed by use of small animal SPECT/CT system (Triumph Lab SPECT4/CT, TriFoil Imaging Inc., Chatsworth, CA) equipped with a five pinhole (0.5 mm) collimator. Data acquisition was performed for 64 min at 240 s per projection with stepwise rotation of 16 projections over 360°.

Conflicts of interest

There are no conflicts to declare.

Acknowledgements

Y. M. was supported by JSPS Research Fellowships for Young Scientists. This work was supported in part by JSPS Research Fellows Program (No. 264896). We thank Prof. Atsushi Nishida

(Chiba University) for valuable discussion on the mechanism of the side reaction.

References

1 C. S. Cutler, H. M. Hennkens, N. Sisay, S. Huclier-Markai and S. S. Jurisson, *Chem. Rev.*, 2013, **113**, 858–883.
2 B. M. Zeglis, J. L. Houghton, M. J. Evans, N. Viola-Villegas and J. S. Lewis, *Inorg. Chem.*, 2014, **53**, 1880–1899.
3 D. Brasse and A. Nonat, *Dalton Trans.*, 2015, **44**, 4845–4858.
4 S. Bhattacharyya and M. Dixit, *Dalton Trans.*, 2011, **40**, 6112–6128.
5 T. J. Wadas, E. H. Wong, G. R. Weisman and C. J. Anderson, *Chem. Rev.*, 2010, **110**, 2858–2902.
6 M. Morais, A. Paulo, L. Gano, I. Santos and J. D. G. Correia, *J. Organomet. Chem.*, 2013, **744**, 125–139.
7 S. Liu, *Adv. Drug Delivery Rev.*, 2008, **60**, 1347–1370.
8 S. Liu and S. Chakraborty, *Dalton Trans.*, 2011, **40**, 6077–6086.
9 J. R. Ballinger, *Q. J. Nucl. Med. Mol. Imaging*, 2002, **46**, 224–232.
10 Y. Mizuno, T. Uehara, H. Hanaoka, Y. Endo, C.-W. Jen and Y. Arano, *J. Med. Chem.*, 2016, **59**, 3331–3339.
11 Y. Mizuno, T. Uehara, H. Hanaoka, Y. Endo, C.-W. Jen and Y. Arano, *J. Med. Chem.*, 2017, **60**, 6768–6769.
12 R. Haubner, H. J. Wester, U. Reuning, R. Senekowitsch-Schmidtke, B. Diefenbach, H. Kessler, G. Stöcklin and M. Schwaiger, *J. Nucl. Med.*, 1999, **40**, 1061–1071.
13 M. Mammen, S. K. Choi and G. M. Whitesides, *Angew. Chem., Int. Ed.*, 1998, **37**, 2754–2794.
14 L. L. Kiessling, J. E. Gestwicki and L. E. Strong, *Curr. Opin. Chem. Biol.*, 2000, **4**, 696–703.
15 S. Bhatia, L. C. Camacho and R. Haag, *J. Am. Chem. Soc.*, 2016, **138**, 8654–8666.
16 Y. Taira, T. Uehara, M. Tsuchiya, H. Takemori, Y. Mizuno, S. Takahashi, H. Suzuki, H. Hanaoka, H. Akizawa and Y. Arano, *Bioconjugate Chem.*, 2018, **29**, 459–466.
17 H. A. Holik, T. Uehara, S. Nemoto, T. Rokugawa, Y. Tomizawa, A. Sakuma, Y. Mizuno, H. Suzuki and Y. Arano, *Bioconjugate Chem.*, 2018, **29**, 2909–2919.
18 X. Chen, Y. Guo, Q. Zhang, G. Hao, H. Jia and B. Liu, *J. Organomet. Chem.*, 2008, **693**, 1822–1828.
19 J. F. Bunnett, *Angew. Chem., Int. Ed. Engl.*, 1962, **1**, 225–235.
20 W. C. Eckelman, A. G. Jones, A. Duatti and R. C. Reba, *Drug Discov. Today*, 2013, **18**, 984–991.
21 W. C. Eckelman, *Eur. J. Nucl. Med. Mol. Imaging*, 1995, **22**, 249–263.
22 K. Sung and C. C. Chen, *Tetrahedron Lett.*, 2001, **42**, 4845–4848.
23 N. Lazarova, S. James, J. Babich and J. Zubieta, *Inorg. Chem. Commun.*, 2004, **7**, 1023–1026.
24 S. M. Creedon, H. K. Crowley and D. G. McCarthy, *J. Chem. Soc., Perkin Trans. 1*, 1998, 1015–1017.
25 R. Alberto, K. Ortner, N. Wheatley, R. Schibli and A. P. Schubiger, *J. Am. Chem. Soc.*, 2001, **123**, 3135–3136.